Absorption Voltages and Insulation Resistance in Ceramic Capacitors with Cracks

Alexander Teverovsky
AS and D, Inc.
7515 Mission Drive, Suite 200, Seabrook, MD 20706
Work performed for NASA Goddard Space Flight Center
8800 Greenbelt Road, Greenbelt, Maryland 20771, USA

ABSTRACT

Time dependence of absorption voltages (V_{abs}) in different types of low-voltage X5R and X7R ceramic capacitors was monitored for a maximum duration of hundred hours after polarization. To evaluate the effect of mechanical defects on V_{abs}, cracks in the dielectric were introduced either mechanically or by thermal shock. The maximum absorption voltage, time to roll-off, and the rate of voltage decrease are shown to depend on the crack-related leakage currents and insulation resistance in the parts. A simple model that is based on the Dow equivalent circuit for capacitors with absorption has been developed to assess the insulation resistance of capacitors. Standard measurements of the insulation resistance, contrary to the measurements based on V_{abs}, are not sensitive to the presence of mechanical defects and fail to reveal capacitors with cracks.

Index Terms: **Ceramic capacitor, insulation resistance, dielectric absorption, cracking.**

I. INTRODUCTION

Multilayer ceramic capacitors (MLCCs) constitute the majority of components used in electronic assemblies. Most of their failures are related to cracks that are caused either by insufficient process control during manufacturing, thermal shock associated with soldering, or flex cracking during handling and/or mechanical testing of the circuit boards. These cracks, if not identified, might cause failures after months and even years of operation. The failure mode varies from a short circuit to intermittent, or "noisy," behavior that in some cases might be misjudged as software failures.

Insulation resistance (IR) is commonly assumed to be a characteristic that is sensitive to the presence of cracks in capacitors. However, polarization currents that are prevailing over the crack-related leakage currents during standard IR measurements, limit the capability of IR testing to screen out defective capacitors. This stimulates the search for new techniques that are effective in revealing capacitors with cracks. As it will be shown below, measurements of absorption voltages in ceramic capacitors may be used for this purpose.

When a pre-charged capacitor is left disconnected after a brief short circuit period, the voltage across the electrodes increases with time. This behavior is due to polarization processes in the dielectric that might include dipole orientation, redistribution of ionic charges, charge injection from electrodes, or electron tunneling into traps in the dielectric [1]. An increase in voltage across a capacitor after a brief short circuit can be explained by the dielectric releasing absorbed charges back to the electrodes. Currents and voltages related to these processes can be defined as absorption currents and absorption voltages, respectively. In technical literature, the phenomenon of voltage recovery is often referred to as the dielectric absorption (DA).

Absorption processes are well known in a variety of dielectric materials employed in different types of capacitors, including MLCCs [2-4]. These processes can limit accuracy and cause errors in analog applications that utilize sample-and-hold circuits, integrating analog-to-digital converters and active filters [5]. DA was also a source of errors in the

voltage-to-frequency transfer circuits of voltage controlled oscillators [6]. In earth sensors for satellites, a charge absorption processes in a capacitor can create spurious signals [7]. To reduce the effect of DA in sensitive applications, designing of special compensating circuits might be necessary [8].

Absorption voltage depends on the polarization conditions (applied voltage and time of polarization), discharge time, and time of recovery. These conditions vary substantially for different applications, and most circuit designers are concerned about the short-term effects of DA [6]. For this reason, the DA method specified in MIL-PRF-19978 (General specification for capacitors) that requires measurement of maximum V_{abs} within 15 minutes, has a limited value. To some degree, this method can be used to assess only a relative capability of different materials for voltage recovery. Most literature data related to V_{abs} were obtained within seconds or minutes after shorting; there is no information on the long-term behavior of absorption voltages in capacitors.

The purpose of this work is to gain insight into long-term absorption processes in low-voltage MLCCs and assess the sensitivity of V_{abs} measurements to the presence of cracks. A simple model based on the equivalent circuit of a capacitor with absorption has been developed to assess the value of the insulation resistance associated with cracks.

II. EXPERIMENT

A variety of MLCCs produced by different vendors were used in this study to reveal common features in absorption currents and voltages. Most of the parts were commercial, high volumetric efficiency, X5R and X7R capacitors [9] with Electronic Industries Alliance (EIA) case size from 0402 to 2225, voltage rating (VR) from 6.3 V to 100 V, and capacitance values from 1500 pF to 100 μF.

Mechanical defects in MLCCs were introduced using three techniques:

- Mechanical fracture. A corner portion of the part was chipped-off using fine cutters (see Fig. 1.a).
- Surface cracking. A capacitor was damaged by impact on the surface with a Vickers indenter (see Fig. 1.b).
- Thermal shock. Capacitors were stressed by a cold thermal shock using the ice water testing technique or hot thermal shock using a solder dip test [10] (see Fig. 1.c and d).

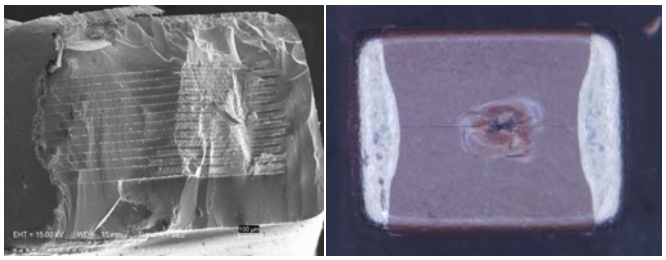

a) b)

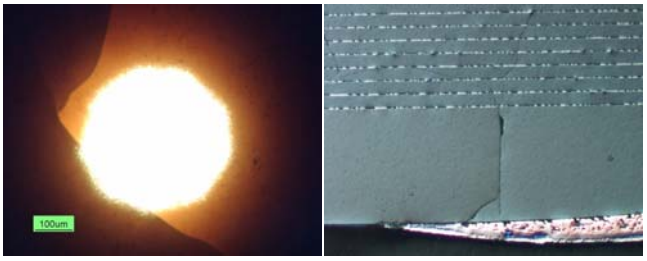

c) d)

Figure 1. Examples of fractured MLCCs. (a) A scanning electron microscope (SEM) view of a chip-out in a case size 2220, 1 μF, 50 V capacitor. (b) Fracture introduced by a Vickers indenter in a case size 1210, 10 μF, 25 V capacitor. (c) A vicinal illumination [11] optical view of cracks on the surface of a case size 2220, 1 μF, 50 V capacitor that were introduced by the ice water thermal shock test. (d) A cross-section of a capacitor with cracks shown in (c).

Absorption voltages were measured using source-measurement units (SMU) manufactured by Keithley (model 236/237) and Agilent (hp4156A). The default procedure for the measurement of V_{abs} in our experiments involved polarization at the rated voltage for one hour, followed by a 5-sec short-circuit period, after which the voltage across the part was recorded with time using a PC-based data acquisition system.

Typical results for measurements of absorption voltages in different types of capacitors are shown in Fig. 2. In all cases, the V_{abs} initially increases relatively quickly, during a few hours or less, reaches maximum, and then decreases slowly over dozens or hundreds of hours. The maximum value of V_{abs} typically varies from 1 V to 3 V and does not correlate with the value of capacitance. In some cases, absorption voltages exceeding 5 V were observed after a few hours of storage for relatively small capacitors in the nano-farad range.

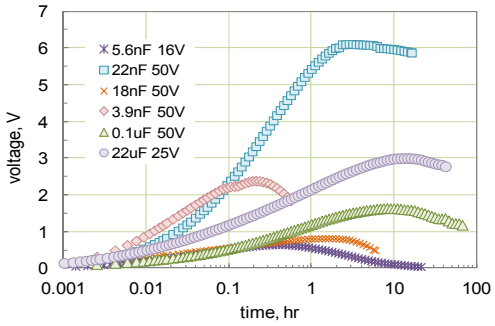

Figure 2. Examples of measurements of absorption voltages in different types of ceramic capacitors.

III. MODELING OF ABSORPTION VOLTAGES

An equivalent circuit of a capacitor (see Fig. 3.a) that accounts for the effects related to dielectric absorption was suggested first for polystyrene capacitors by Dow in 1958 [12] and expanded recently using a Col-Cole dielectric permittivity model by Kundert [13]. The capacitor has a nominal value C_0 and insulation resistance R. Dow showed that most absorption polarization processes in capacitors can be described using a circuit with five r-C_t relaxators connected in parallel to C_0 by a proper selection of the

relaxation times, $\tau_i = r_i \times C_{ti}$, and absorption capacitances C_{ti}.

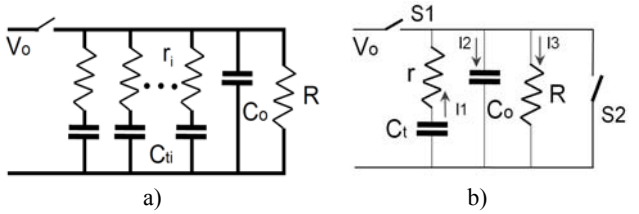

a) b)

Figure 3. Equivalent circuit of capacitors with absorption. (a) A Dow model. (b) A model for calculations of absorption voltages. Direction of currents I1, I2, and I3 are shown for a case when both switches, S1 and S2, are open.

If a capacitor that is modeled by the circuit shown in Fig. 3.a remains under bias for a long period of time (exceeding the maximum characteristic time τ_i), then each of the capacitors C_{ti} will be charged to V_0. Shorting for a period of Δt will discharge only C_0, and capacitors C_{ti} associated with relatively fast r_i-C_{ti} relaxators that have $\tau_i < \Delta t$. All other capacitors will remain charged, and when the circuit is open, these charges will leak out to C_0 and increase the voltage across the capacitor. This voltage will increase with time until discharging currents through the leakage resistor R prevail, thus resulting in the voltage roll-off. The absorption voltage will decrease with time, and eventually the capacitor will discharge completely.

When the absorption voltage is decreasing with time, the process is scaled to the characteristic time related to the capacitor resistance R, $\tau_0 = R \times C_0$. By this time, relaxators with $\tau_i << \tau_0$ will be mostly discharged. Considering that the charging period is less than τ_0, relaxators with $\tau_i >> \tau_0$ have practically no charge, and will not contribute substantially to the discharging process. For this reason, we can simplify the equivalent circuit, Fig. 3.a, by considering only one relaxator that has timing characteristics within orders of magnitude of the duration of polarization.

Let us consider the schematic of a capacitor shown in Fig. 3.b that had been pre-charged for some time (switch S1 closed and S2 open) and then short-circuited briefly (switch S1 open and S2 closed). At the end of the pre-charge period, the voltage across capacitor C_t was U_0 and due to a large value of resistor r, it did not change substantially during the short circuit period.

From the first Kirchhoff's law:

$$i_1 = i_2 + i_3 , \tag{1}$$

Where the currents can be expressed as follows:

$$i_1 = -C_t \frac{du}{dt}, \quad i_2 = C_0 \frac{dv}{dt}, \quad i_3 = \frac{v}{R} . \tag{2}$$

Here $u(t)$ is the voltage across the capacitor C_t, and $v(t)$ is the absorption voltage, or voltage across C_0.

The balance of currents, Eq.(1), can be written as:

$$-C_t \frac{du}{dt} = C_0 \frac{dv}{dt} + \frac{v}{R} , \tag{3}$$

The voltage across C_0 is less than across C_t due to a voltage drop on the resistor r:

$$v(t) = u(t) - i_1 \times r . \tag{4}$$

After a substitution for currents per Eq.(2) the derivative of Eq.(1) and Eq.(4) can be presented as:

$$\frac{d^2u}{dt^2} = -\frac{1}{C_t R}\frac{dv}{dt} - \frac{C_0}{C_t}\frac{d^2v}{dt^2} , \tag{5}$$

$$\frac{dv}{dt} = C_t \times r \times \frac{d^2u}{dt^2} + \frac{du}{dt} , \tag{6}$$

Substitution of Eq.(3) and Eq.(5) into Eq.(6) gives an equation for the absorption voltage:

$$a\frac{d^2v}{dt^2} + b\frac{dv}{dt} + c \times v = 0 , \tag{7}$$

where

$$a = \tau_0 \frac{\tau}{\tau_t}, \quad b = \frac{\tau + \tau_t + \tau_0}{\tau_t}, \quad c = \frac{1}{\tau_t}$$

are constants, and

$$\tau = r \times C_t, \quad \tau_0 = R \times C_0, \quad \tau_t = R \times C_t ,$$

are the characteristic times of the charge distribution processes.

The general solution to Eq.(7) for the variations of the voltage across the capacitor C_0 with time after switch S2 is open can be written in the form:

$$v(t) = A \times \exp(x_1 \times t) + B \times \exp(x_2 \times t), \tag{8}$$

Constants $x_{1,2}$ are solutions of the relevant characteristic equation:

$$x_{1,2} = \frac{-b \pm \sqrt{b^2 - 4ac}}{2a} ,$$

Constants A and B can be found from the initial conditions:

$$v(0) = 0 \quad \text{and} \quad \left.\frac{dv}{dt}\right|_0 = \frac{U_0}{r \times C_0} ,$$

After substitutions:

$$A = -B = \frac{U_0}{r \times C_0 \times (x_1 - x_2)}$$

Out of the three model parameters, r and R can be found from the best-fit approximation of the $V_{abs}(t)$ curves after roll-off, and C_t can be estimated independently. The absorption capacitance was calculated as a ratio of the charge, Q_t, that is transferred into the dielectric during polarization and applied voltage, $C_t = Q_t/V$. The value of Q_t was calculated by integrating of the absorption current with time of polarization.

Variations of Q_t with voltage for 4 types of capacitors are shown in Fig. 4. Results show that the charge increases with voltage linearly, so the slopes of the lines allow for estimations of C_t. The value of C_t is comparable to the nominal value of the capacitors and varies from 0.6 μF, for 2.2 μF capacitors, to 39 μF, for 100 μF capacitors.

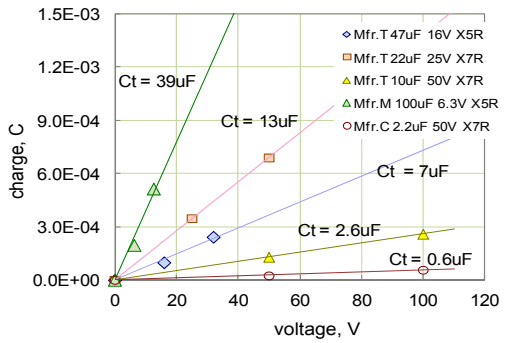

Figure 4. Variations of absorption charges in different types of EIA2220, X7R/X5R MLCCs. The absorption capacitance (C_t) was calculated as the slope of the $Q_t - V$ lines.

Absorption capacitance was found to be greater for larger valued capacitors. A correlation between the standard capacitance value, C_0, that is measured at 1 kHz, and absorption capacitance, C_t is shown in Fig. 5. For most capacitors, C_t values were in the range from 10% to 50% of the nominal value. On average, $C_t \sim 0.3 \times C_0$.

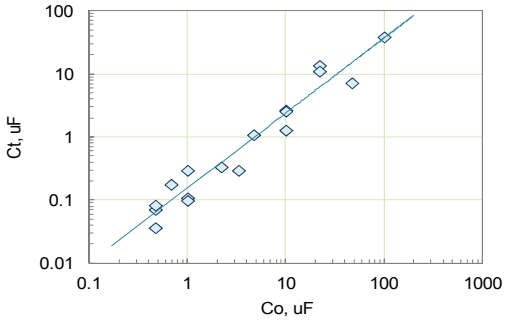

Figure 5. Correlation between the absorption and nominal values of capacitance for 17 different types of X7R MLCCs.

To evaluate how variations of different parameters of the model affect absorption voltages, let us consider a 1 μF, 10 V capacitor that was pre-charged at a rated voltage for a long time, so U_0 = 10 V. The part was then discharged for a few seconds, and V_{abs} was monitored with time using a voltmeter with an internal resistance that exceeds substantially the resistance associated with the leakage current. Assuming that the leakage resistance, R, is 10^{10} Ω (a typical IR requirement for ceramic capacitors) and the resistance of the relaxator, r, is 10^8 Ω, the effect of variation of the absorption capacitance, C_t in the range from $0.1 \times C_0$ to C_0 on the $V_{abs}(t)$, is shown in Fig. 6.a. As expected, the amplitude of V_{abs} increases with C_t; however, the raise occurs sublinearly, and at $r << R$ can be approximated with a simple function that is derived based on the charge redistribution from C_t to $(C_t + C_0)$:

$$V_{max} = U_0 \times C_t/(C_t + C_0). \quad (9)$$

The effect of the resistance of the relaxator, r, for a capacitor having $R = 10^{12}$ Ω and C_t = 0.5 μF is shown in Fig. 6.b. Increasing r from 10^8 Ω to 10^{12} Ω affects mostly the time of the voltage onset, whereas the decreasing portion of the curve remains practically unchanged.

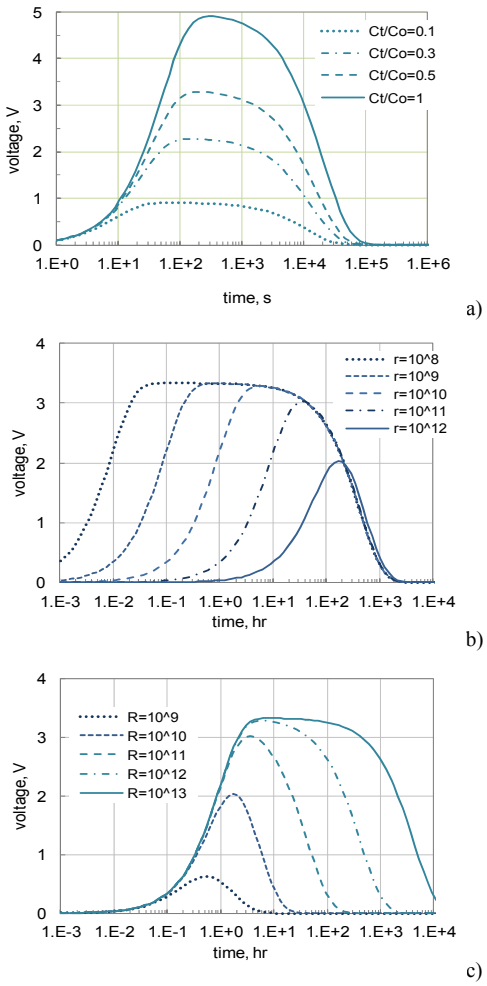

Figure 6. Simulation of absorption voltages for 1 μF, 10 V capacitor. (a) Effect of absorption capacitance, C_t, at $r = 10^8$ ohm and $R = 10^{10}$ ohm. (b) Effect of the relaxator resistance, r, at C_t = 0.5 μF and $R = 10^{12}$ ohm. (c) Effect of the insulation resistances, R, at $r = 10^{10}$ ohm and C_t = 0.5 μF.

For a case when the resistance of the relaxator is constant, $r = 10^{10}$ Ω, and the resistance related to leakage currents, R, varies from 10^9 Ω to 10^{13} Ω, the kinetics of the variation of absorption voltages are shown in Fig. 6.c. At R exceeding r, the amplitude of V_{abs} remains constant, but the time to roll-off increases with R substantially.

Simulations showed that the time to roll-off and the rate of the voltage decrease depend strongly on the value of R, and that long-term variations of V_{abs} can be used to estimate the insulation resistance of capacitors.

IV. TEST RESULTS

Examples of $V_{abs}(t)$ characteristics measured for two samples of 10 μF, 25 V capacitors are shown in Fig. 7. Similar results were obtained for other types of capacitors and indicate a high reproducibility of V_{abs} measurements from sample to sample. Except for the initial part of the curve, where V_{abs} is rising, time dependence of the absorption voltage is in agreement with the model described in the previous section. The discrepancy will be explained in the next section. Dashed lines shown in Fig. 7, and the following

charts, are calculations per Eq.(8) using the best-fit approximation and parameters adjustment technique. Based on measurements of the absorption capacitance for 10 μF, 25 V capacitors, $C_t = 0.15 \times C_0$. The best-fit approximation resulted in $r = 2 \times 10^9$ Ω and $R = 2 \times 10^{10}$ Ω.

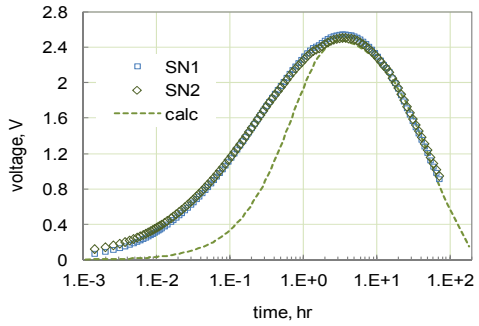

Figure 7. Variations of absorption voltages for two samples of 10 μF, 25 V, case size 1210 capacitors.

Experiments showed that an increase in voltage during polarization enlarges absorption voltages. Fig. 8.a shows the effect of polarization voltage on 3.3 μF, 6.3 V capacitors at polarization voltages varying from VR to 4×VR. In all cases, experimental data were approximated with $V_{abs}(t)$ curves calculated at values of C_t =0.4 μF, $r = 10^{10}$ Ω and $R = 5 \times 10^{11}$ Ω.

Fig. 8.b shows variations of the maximum V_{abs} with the polarization voltage normalized to the rated voltage for three types of MLCCs. The maximum value of V_{abs} increases linearly at low voltages and saturates at high voltages, following a trend that typically exceeds the rated voltage by 2 to 3 times.

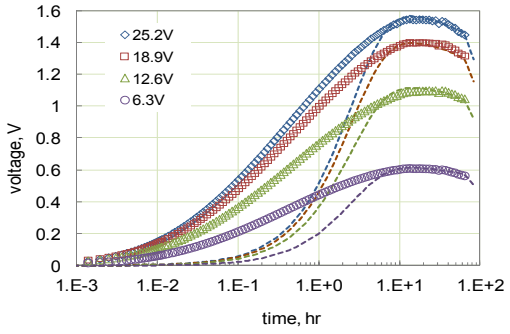

a)

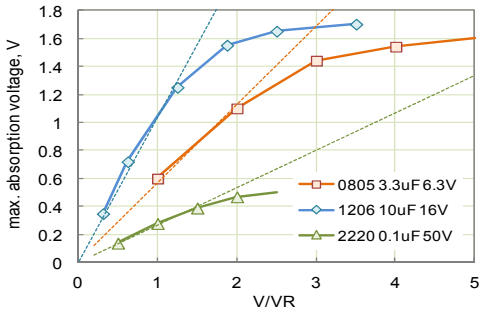

b)

Figure 8. Effect of polarization voltage on absorption voltages. (a) Case size 0805, 3.3 μF, 6.3 V capacitor; C_t =0.4 μF, $r = 10^{10}$ ohm and $R = 5 \times 10^{11}$ ohm. (b) Variation of the maximum V_{abs} with polarization voltage normalized to VR.

A comparison of $V_{abs}(t)$ curves for capacitors in normal conditions and after cracking, introduced either by the Vickers indenter or mechanical fracture, is shown in Fig. 9. In the damaged capacitors, a decrease of V_{abs} occurs much earlier, and because the cracks in different parts can not be duplicated, the reproducibility of test results is less than was found for normal parts. For 1 μF, 50 V capacitors (Fig. 9.a), the calculated resistance dropped from the initial 3×10^{13} Ω to ~2×10^{12} Ω, after cracking. In all cases, the model parameters used for calculations were C_t = 0.35 μF and $r = 2 \times 10^{11}$ Ω. For 0.1 μF, 100V capacitors (Fig. 9.b), R decreased by 2 to 4 orders of magnitude: from more than 5×10^{14} Ω initially to either 2.5×10^{12} Ω or 7×10^{10} Ω, depending on the fractured samples. The parameters used for these calculations were: C_t = 9 nF and $r = 10^{11}$ Ω. Note that in all cases, fractured capacitors had values of R exceeding the requirements specified for insulation resistance.

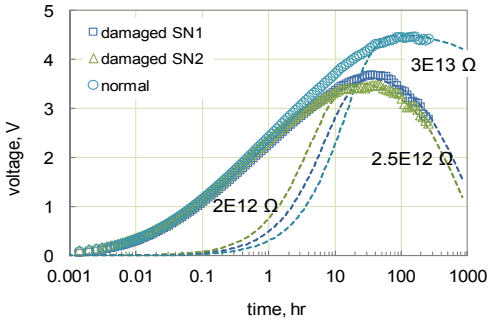

a)

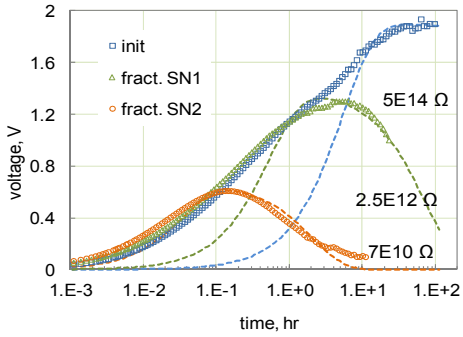

b)

Figure 9. Absorption voltages in normal and damaged capacitors. Dashed lines are calculations per Eq.(8) at indicated values of the insulation resistance. (a) Case size 1812, 1 μF, 50 V capacitors damaged by a Vickers indenter. (b) Case size 1825, 0.1 μF, 100 V capacitor, mechanically fractured.

Two types of thermal shock, the ice water test and the solder dip test, were used to evaluate the effect of cracking on absorption voltages in large-size (EIA 2220) 10 μF, 50 V and 1 μF, 50 V capacitors. Results of these tests are shown in Fig. 10. For 10 μF capacitors, the initial value of the resistance was 5×10^{13} Ω, and after fracture, R was reduced to 3×10^{10} Ω (the model parameters were: C_t = 3 μF, $r = 10^{10}$ Ω). The difference was less dramatic for 1 μF capacitors, but still the resistance decreased an order of magnitude: from 3×10^{12} Ω to 3×10^{11} Ω (C_t = 0.13 μF, $r = 1.5 \times 10^{11}$ Ω).

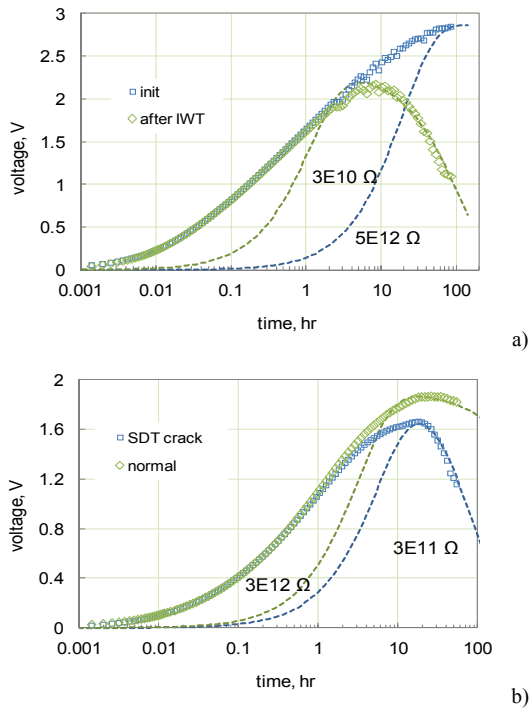

Figure 10. Effect of cracking caused by thermal shock on absorption voltages in two types of case 2220 ceramic capacitors. (a) 10 μF, 50 V capacitor damaged by ice water thermal shock. (b) 1 μF, 50 V capacitor, damaged by solder dip thermal shock (SDT).

The effect of fracture on resistance values that were calculated based on the $V_{abs}(t)$ curves, before and after mechanical damage, for 20 different types of capacitors, is shown in Fig. 11. In 70% of the cases, a substantial (more than 2-times) decrease of R, due to cracking, was observed. The resistance in capacitors with cracks remained rather large, typically exceeding 10^9 ohm, and was above the specified values.

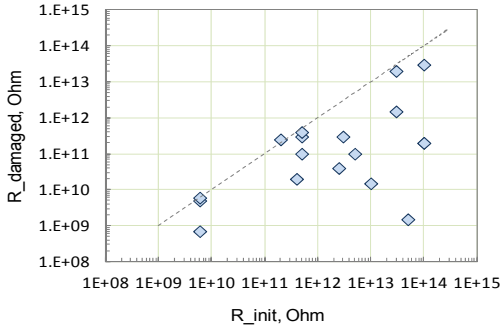

Figure 11. Effect of fracturing on the value of resistance, calculated based on absorption voltage measurements, in 20 different types of capacitors. Dashed line corresponds to no-change values.

V. DISCUSSION

Long-term variations of V_{abs} were in reasonable agreement with the model shown in Fig. 3.b. During relatively short periods of time, the discrepancy was large because the parameters of the model were chosen to fit experimental data both at maximum V_{abs} and after the voltage roll-off. The initial portion of the curve cannot be accurately described with a single r-C_t relaxator and requires additional analysis that is out of scope of this paper.

For normal and damaged capacitors, an initial increase of V_{abs} was similar, which is consistent with the model. The initial variation of absorption voltages are controlled by C_0, C_t, and r, and do not depend on the insulation resistance. However, the maximum value of V_{abs}, time to roll-off, and the rate of voltage decrease with time depend on R and are sensitive to variations of the intrinsic leakage currents caused by the presence of cracks. The voltage absorption measurement technique essentially measures an integral of leakage currents accumulated on the capacitor C_0:

$$v(t) = \int_0^t \frac{I_1(t) - I_3(t)}{C_0} dt, \qquad (10)$$

where $I_1(t)$ is the discharge current from C_t, and $I_3(t)$ is the leakage current (see Fig. 3.b).

In exchange for the price of long-duration measurements, estimations of large insulation resistances are achievable: up to 10^{14} Ω. Also, there is no need of application of high voltages that are usually required to measure high resistances.

The maximum value of V_{abs} increases linearly with polarization voltage at applied voltages less than 2×VR to 3×VR, and has a tendency to saturate at larger voltages (see Fig. 8.b). This might be attributed to the non-linearity of the elements used in the model. In X5R and X7R materials, the capacitance is known to decrease with voltage. However, at a constant C_t, a decrease of C_0 with voltage would increase V_{abs}. This is because the same amount of charge accumulated at C_t would be distributed to a lesser capacitance. For this reason, explaining the saturation of V_{abs} with the non-linearity of C_0 should be excluded. Assuming that the charge absorption and desorption (release) processes are due to electron trapping in electron states (traps) [1], for example, at the grain boundaries of the ceramic [14], it is possible to explain the saturation of V_{abs} by a limited amount of the available traps. As soon as all traps are filled with electrons, an additional voltage increase would not increase the trapped charge, and hence would not increase the maximum V_{abs}.

Experiments showed that the maximum value of V_{abs} does not depend on the value of capacitance, and remains within a few volts for different part types. According to the model, absorption voltage depends on the ratio of C_t/C_0, rather than on the nominal value of capacitance. Considering that the ratio C_t/C_0 remains within a rather narrow range, from 10% to 50%, variations of the maximum value of V_{abs} for different part types is also relatively small.

In most cases (~70% out of 20 tested parts), cracking resulted in a noticeable decrease of the resistance, suggesting that this technique can be used to reveal capacitors with defects. In several cases that were related to high volumetric efficiency capacitors, no decrease in the resistance after damage was due to the capacitor's initial low resistance. In these cases, the intrinsic leakage current exceeded the damage-related currents, thus masking the presence of the defects. In other cases, the damage was introduced by the

indenter, and most likely the cracks were not large enough to penetrate into the active area of the capacitors.

To evaluate the effectiveness of the standard IR measurements in revealing cracks, insulation resistances for 15 different types of MLCCs were measured before and after mechanical fracture. According to the standard technique, IR measurements should be made within 120 seconds of electrification at the rated voltage, $IR = VR/I_{120}$. Results of these measurements are shown in Fig. 12. The range of IR for normal quality parts was from 10^7 Ω to 3×10^{11} Ω, which is within the specified limits. Mechanical damage did not change the resistance substantially, thus indicating a failure of standard IR testing to reveal cracks in capacitors.

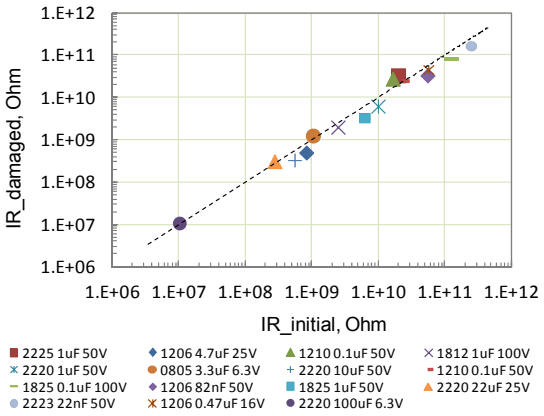

Figure 12. Effect of cracking on insulation resistance in 15 different types of ceramic capacitors. The IR measurements were carried out using a standard technique: 120 seconds of electrification at rated voltages. The dashed line corresponds to no-change values.

This result can be explained by considering that polarization, or absorption currents, are typically significantly greater than the leakage currents related to the presence of cracks. This is also clear from an analysis of the equivalent circuit, shown in Fig. 3.b. When a voltage, V_0, is applied (switch S2 open and S1 closed), variations of the current with time can be presented as the sum of the leakage and absorption currents:

$$I(t) = \frac{V_0}{R} + \frac{V_0}{r}\exp\left(-t/r\times C_t\right) \qquad (11)$$

At $r << R$, and relatively small time intervals after voltage application, $t < (r\times C_t)\times\ln(R/r)$, the absorption currents prevail over the leakage currents (V_0/R) and the results of IR measurements are not sensitive to the presence of defects. For this reason, measurements of insulation resistances using the absorption voltage technique, instead of measuring absorption currents with the standard method, result in values of R that are almost three orders of magnitude greater.

In most cases, the maximum V_{abs} exceeded 1 or 2 volts, and the capacitor might remain at voltages above 1 V even after hundreds of hours of storage in room conditions. The presence of this voltage across capacitors during storage might initiate degradation processes similar to those that cause failures in capacitors with defects during low-voltage humidity testing. Several cases of failures in ceramic capacitors after long-term storage have been reported. Holladay [15] observed 5 failures in a group of 100 capacitors (1.2 μF, 100 V) stored on the shelf for 2 years at room ambient. These parts had IR ~1.5×10^4 Ω at 2V, but the value jumped to ~3×10^8 Ω at 16V, which is typical for the low-voltage failure phenomenon. Three out of 30 virgin military-grade 47 nF, 100 V capacitors from a lot suspected to be defective and causing failures in hybrids were found to be "leaky" during initial testing [16]. Assuming that all of the capacitors manufactured to military specifications were non-defective originally, the observed 10% failures can be ascribed as a storage-induced degradation. Improvements in the testing techniques, in particular using the suggested voltage absorption test method, would reduce the probability that defective parts escape the screening.

VI. Conclusion

1. Absorption voltages in X5R and X7R MLCCs typically increase within a few hours after polarization at VR, up to several volts. Subsequently, V_{abs} decreases slowly and can remain above one volt even after hundreds of hours. The maximum value of V_{abs} does not correlate with the value of capacitance, increases linearly with polarization voltages below ~3×VR, and stabilizes at greater voltages.
2. The time to roll-off for V_{abs} and the rate of voltage decrease are related to the leakage currents in the capacitors. A simple model that is based on the Dow equivalent circuit for capacitors with absorption has been developed to explain long-term variations of absorption voltages and estimate insulation resistances in MLCCs.
3. The suggested method that is based on monitoring long-term variations of V_{abs} allows for estimations of the insulation resistances up to 10^{14} Ω. Measurements of insulation resistance in MLCCs using a standard technique fail to reveal capacitors with cracks, whereas the voltage absorption technique was effective in more than 70% of cases.

VII. Acknowledgment

This work was sponsored by the NASA Electronic Parts and Packaging (NEPP) program. The author is thankful to Michael Sampson, NEPP Program Manager, for support of this investigation, and to Jaemi Herzberger (UMCP) for assistance with preparing the manuscript.

VIII. References

[1] G. G. Raju, "*Dielectrics in electric fields*": CRC Press, Marcel Dekker, p. 592, 2003.

[2] X. Xu, M. Niskala, A. Gurav, M. Laps, and K. Saarinen, "Advances in Class-I C0G MLCC and SMD Film Capacitors," in *The 27th symposium for passive components, CARTS'07*, Newport Beach, CA, pp.36-42, 2007.

[3] H. Bachhofer, H. Reisinger, H. Schroeder, T. Haneder, C. Dehm, H. Von Philipsborn, and R. Waser, "Relaxation effects and steady-state conduction in non-stoichiometric SBT films," *Integrated Ferroelectrics*, vol. 33, pp. 245-252, 2001.

[4] H. Y. Lee, K. C. Lee, J. N. Schunke, and L. C. Burton, "Leakage currents in multilayer ceramic capacitors," *IEEE Transactions on Components Hybrids and Manufacturing Technology,* vol. 7, pp. 443-453, 1984.
[5] B. Pease. "Understand Capacitor Soakage to Optimize Analog Systems", 1982 *EDN*. Available: http://www.national.com/rap/Application/0,1570,28,00.html
[6] J. C. Kuenen and G. C. M. Meijer, "Measurement of dielectric absorption of capacitors and analysis of its effects on VCOs," *Instrumentation and Measurement, IEEE Transactions on,* vol. 45, pp. 89-97, 1996.
[7] J. Burnham, S. L. Webster, W. J. Simmons, and J. W. Borough, "A Study of Dielectric Absorption in Capacitors by Thermally Stimulated Discharge (TSD) Tests," in *Reliability Physics Symposium, 1976. 14th Annual*, 1976, pp. 147-156.
[8] C. Iorga, "Compartmental analysis of dielectric absorption in capacitors," *Dielectrics and Electrical Insulation, IEEE Transactions on,* vol. 7, pp. 187-192, 2000.
[9] IEA Standard: "Ceramic Dielectric Capacitors Classes I, II, III and IV – Part I: Characteristics and Requirements", EIA-198-1-F, Electronic components, assemblies and materials association, 2002
[10] A. Teverovsky, "Thermal Shock Testing and Fracturing of MLCCs under Manual Soldering Conditions," *IEEE Transactions on Device and Materials Reliability* vol. 12, pp. 413-419, 2012.
[11] S. Hull, "Nondestructive detection of cracks in ceramics using vicinal illumination," in *25th International Symposium for Testing and Failure Analysis, ISTFA*, Santa Clara, CA, 1999, pp. 217-223.
[12] P. C. Dow, "An Analysis of Certain Errors in Electronic Differential Analyzers II-Capacitor Dielectric Absorption," *Electronic Computers, IRE Transactions on,* vol. EC-7, pp. 17-22, 1958.
[13] K. Kundert, "Modeling Dielectric Absorption in Capacitors", 2008 *The designer's guide community,* pp. 1-19. Available: http://www.designers-guide.org/Modeling/da.pdf
[14] L. C. Burton, "Voltage dependence of activation energy for multilayer ceramic capacitors," *Ieee Transactions on Components Hybrids and Manufacturing Technology,* vol. 8, pp. 517-524, Dec 1985.
[15] A. M. Holladay, "Unstable insulation resistance in ceramic capacitors " *Proceedings of Capacitor Technologies, Applications and Reliability, NASA,* pp. 27-31, 1981.
[16] M. Sampson, J. Brusse, and A. Teverovsky, "Humidity Steady State Low Voltage Testing of MLCCs (Based on NESC Technical Assessment Report)," in *CARTS USA, The 31th symposium for passive components,* Jacksonville, Fl, pp. 12-18, 2011.